LAWRENCE
LIVERMORE
NATIONAL
LABORATORY

LLNL-CONF-432812

Simulation of Combustion of C/B Clouds in Explosions

A. L. Kuhl, J. B. Bell, V. E. Beckner

May 20, 2010

DoD High performance Computing Users Group Meeting
Schaumburg, IL, United States
July 14, 2007 through July 17, 2010

Disclaimer

This document was prepared as an account of work sponsored by an agency of the United States government. Neither the United States government nor Lawrence Livermore National Security, LLC, nor any of their employees makes any warranty, expressed or implied, or assumes any legal liability or responsibility for the accuracy, completeness, or usefulness of any information, apparatus, product, or process disclosed, or represents that its use would not infringe privately owned rights. Reference herein to any specific commercial product, process, or service by trade name, trademark, manufacturer, or otherwise does not necessarily constitute or imply its endorsement, recommendation, or favoring by the United States government or Lawrence Livermore National Security, LLC. The views and opinions of authors expressed herein do not necessarily state or reflect those of the United States government or Lawrence Livermore National Security, LLC, and shall not be used for advertising or product endorsement purposes.

Simulation of Combustion of C/B Clouds in Explosions[‡]

Allen L. Kuhl
Lawrence Livermore National Laboratory, Livermore, CA
kuhl2@llnl.gov

John B. Bell and Vincent E. Beckner
Lawrence Berkeley National Laboratory, Berkeley, CA
{jbbell, vebeckner}@lbl.gov

Abstract

We have developed adaptive high-resolution methods for numerical simulations of turbulent combustion of chemical/biological (C/B) clouds in thermobaric explosions. The code is based on our AMR (Adaptive Mesh Refinement) technology that was used successfully to simulate distributed energy release in explosions, such as: afterburning in TNT explosions and turbulent combustion of Shock-Dispersed-Fuel (SDF) charges in confined explosions. Versions of the methodology specialized for low-Mach-number flows have also been developed and extensively validated on a number of laboratory-scale laminar and turbulent flames configurations. In our formulation, we model the gas phase by the multi-component form of the reacting gasdynamics equations, while the particle phase is modeled by continuum mechanics laws for 2-phase reacting flows, as formulated by Nigmatulin. Mass, momentum and energy interchange between phases are taken into account using Khasainov's model. Both the gas- and particle-phase conservation laws are integrated with their own second-order Godunov algorithms that incorporate the non-linear wave structure associated with such hyperbolic systems. Specialized ODE methods are used to integrate chemical kinetics and interphase terms. Adaptive grid methods are used to capture the energy-bearing scales of the turbulent flow (the MILES approach of J. Boris) without resorting to traditional turbulence models. The code is built on an AMR framework that manages the grid hierarchy. Our work-based load-balancing algorithm is designed to run efficiently on massively parallel computers[**]. Gas-phase combustion in the explosion-products (EP) cloud is modeled in the fast-chemistry limit, while Aluminum particle combustion in the EP cloud is based on the finite-rate empirical burning law of Ingignoli. The thermodynamic properties of the components are specified by the Cheetah code. At the 6th HPCUG meeting in 2009, we summarized recent progress in: "AMR Code Simulations of Turbulent Combustion in Confined and Unconfined SDF Explosions". These models were used successfully to simulate the simultaneous after-burning of booster products and combustion of Al in SDF explosion clouds. Computed pressure histories were shown to be in excellent agreement with the data—thereby proving the validity of our combustion modeling of such explosions. This year, the modeling has been extended to include the mixing and combustion of C/B clouds in such explosion fields. Here we will establish how the cloud consumption by combustion depends on chamber environments.

1. Introduction

We have studied distributed energy release in confined explosions as a Grand Challenge Project of the DoD High Performance Computing Modernization Program. Laboratory experiments were performed with 1.5-gram Shock-Dispersed-Fuel (SDF) charges [1]. The charge consisted of a 0.5-g PETN booster surrounded by 1-g of flake Aluminum (Al) powder. The SDF charge was placed at the center of a bomb calorimeter. Detonation of the booster disperses the fuel, ignites it, and induces an exothermic energy release via a turbulent combustion process. Over-pressure histories in air were considerably larger than those measured in nitrogen atmospheres; impulses histories show factors of 2 to 4 increase due to Al-air combustion.

At the *4th HPCMP Users Group Meeting* in 2007, we described our two-phase AMR code that we have used to simulate the distributed energy release in such SDF explosions [2]. We model the flow field as a dilute heterogeneous continuum—with separate conservation laws for each phase—and interaction terms that allow the phases to exchange mass, momentum and energy via phenomenological laws. A unique feature of the model is that a

[**] *Weak Scaling* has been demonstrated for up to 65,000 processors on the Jaguar Cray XT5 machine at Oakridge, TN.

[‡] Approved for public release; distribution is unlimited. LLNL-CONF-413615

high-order Godunov algorithm is used not only for the gas phase, but also for the particle phase. This provides an accurate solution of the governing hyperbolic conservation laws that is devoid of artificial effects of numerical diffusion. The system of equations is closed by a quadratic EOS model, that specifies the thermodynamic states of the combustion fields.

At the 6^{th} *HPCUG* meeting in 2009, we summarized recent progress in "AMR Code Simulations of Turbulent Combustion in Confined and Unconfined SDF Explosions" [3]. These models were used successfully to simulate the simultaneous after-burning of booster products and combustion of Al in SDF explosion clouds. A cross-sectional view of the computed temerature field of the Al-air combustion cloud is presented in Fig. 1. Computed pressure histories (Fig. 2) are in excellent agreement with the data—thereby proving the validity of our combustion modeling of such explosions.

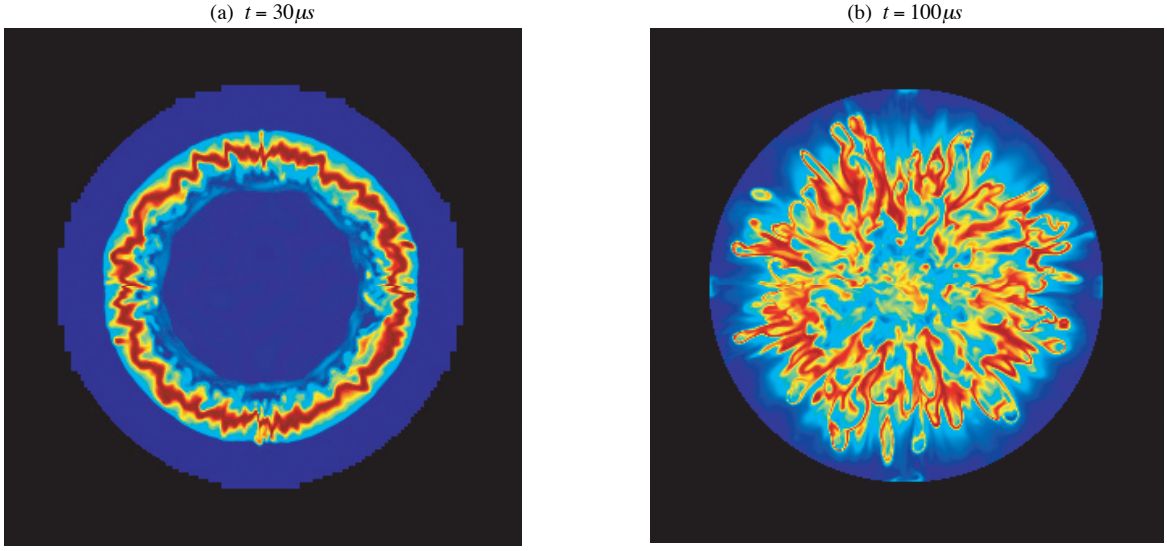

Figure 1. Cross-sectional view (z = 10 cm) of the temperature fields for the Al-air combustion cloud in calorimeter A.

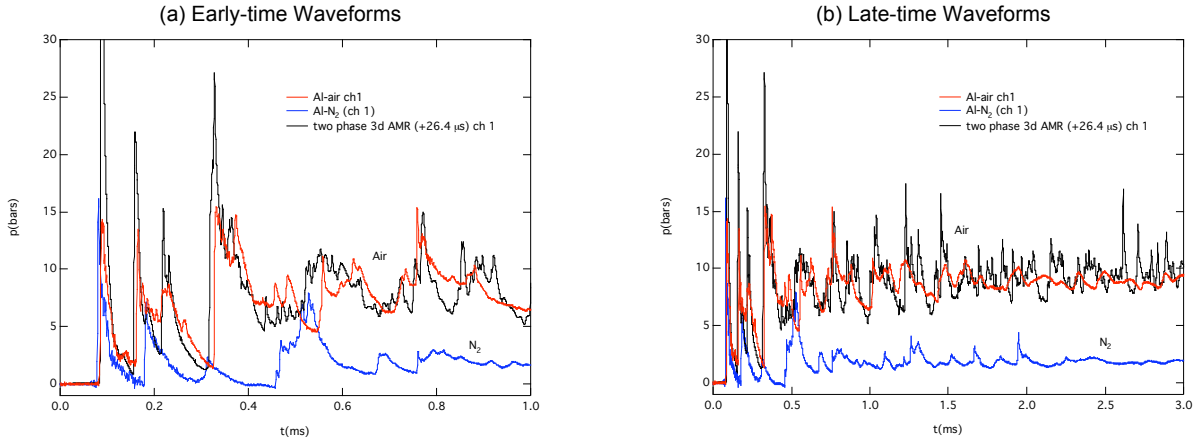

Figure 2. Pressure histories corresponding to 1.5-g Al-SDF charge explosion in calorimeter A.

This year, the modeling has been extended to include the mixing and combustion of Chemical/Bilological (C/B) agents in such explosion clouds. Here we will establish how the agent consumption by combustion depends on chamber environments from conventional and thermobaric charges. An overview of benchmark experiments on the ignition and combustion of simulated C/B clouds in a tunnel are presented in **§2**. The heterogeneous continuum model (including the conservation laws, interphase interactions, combustion model, equations of state and numerical methods) is described in **§3**. The model was used to simulate the evolution of combustion in the aforementioned experiments; results are presented in **§4**. This is followed by conclusions in **§5.**

2. Experiments

Chemical agents (e.g., organo-fluro-carbons) typically decompose into hydrocarbons (CH_3, C_3H_6, etc.), hydrogen fluoride and phosphorus oxide at temperatures above 200 C [4]. The exothermic (explosive) characteristics may be studied as combustion of hydrocarbons with air. To that end, a 4-liter rectangular test chamber (10.15 cm x 10.15 cm x 38.6 cm) was constructed (Fig. 3). Optical (Makrolon) windows were used as the front and back walls to visualize the flow field of the explosion. An explosive charge (e.g., 0.5-g spherical PETN charge, or a 1.5-g SDF charge) was located at x = 9.65 cm. A spherical hydrocarbon cloud was located at x = 26. 8 cm. The cloud was contained in a soap bubble filled with hydrocarbon gas (e.g., acetylene, butane or propane) [5].

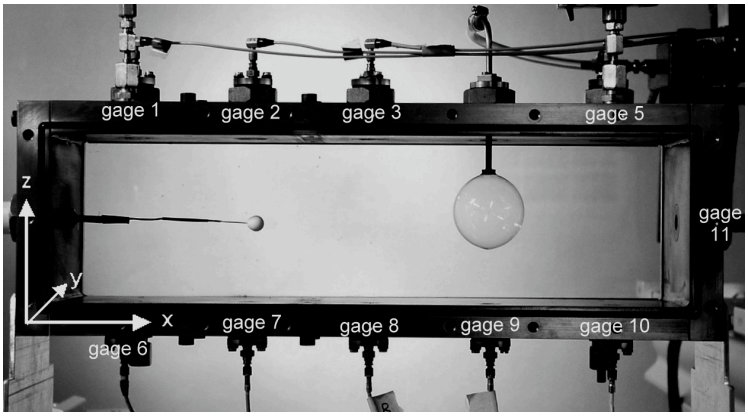

Figure 3. Rectangular test chamber with a 0.5-g PETN charge and a hydrocarbon cloud (d = 5 cm).

Figure 4 provides a sequence of shadow photographs to visualize the blast wave from the HE charge and its interaction with the soap bubble. The shock wave crushes the bubble and deposites vorticity on the bubble surface, leading to mixing of the cloud gases with the blast wave gases, ignition and combustion of the cloud with air [5].

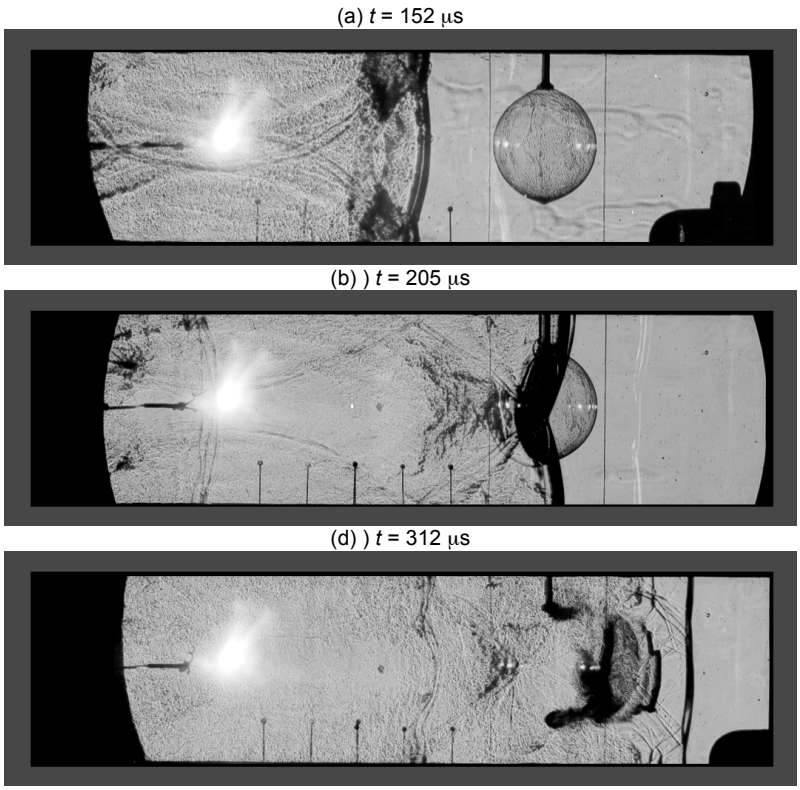

Figure 4. Shadow photographs of the blast wave from a 0.3-g PETN charge and its interactions with a 55-mm soap bubble (air).

Figure 5 shows a sequence of pseudo-color high-speed photographs depicting the hot detonation and combustion products in the chamber [5]. Test conditions are: 50-mm acetylene bubble subjected to a 0.2-g charge at x = 13 cm. With exception of black (setup contours) and blue (background), colors correspond to temperatures above ~700°C. At t = 4.55 ms we find the first indication of acetylene combustion (red cloud).

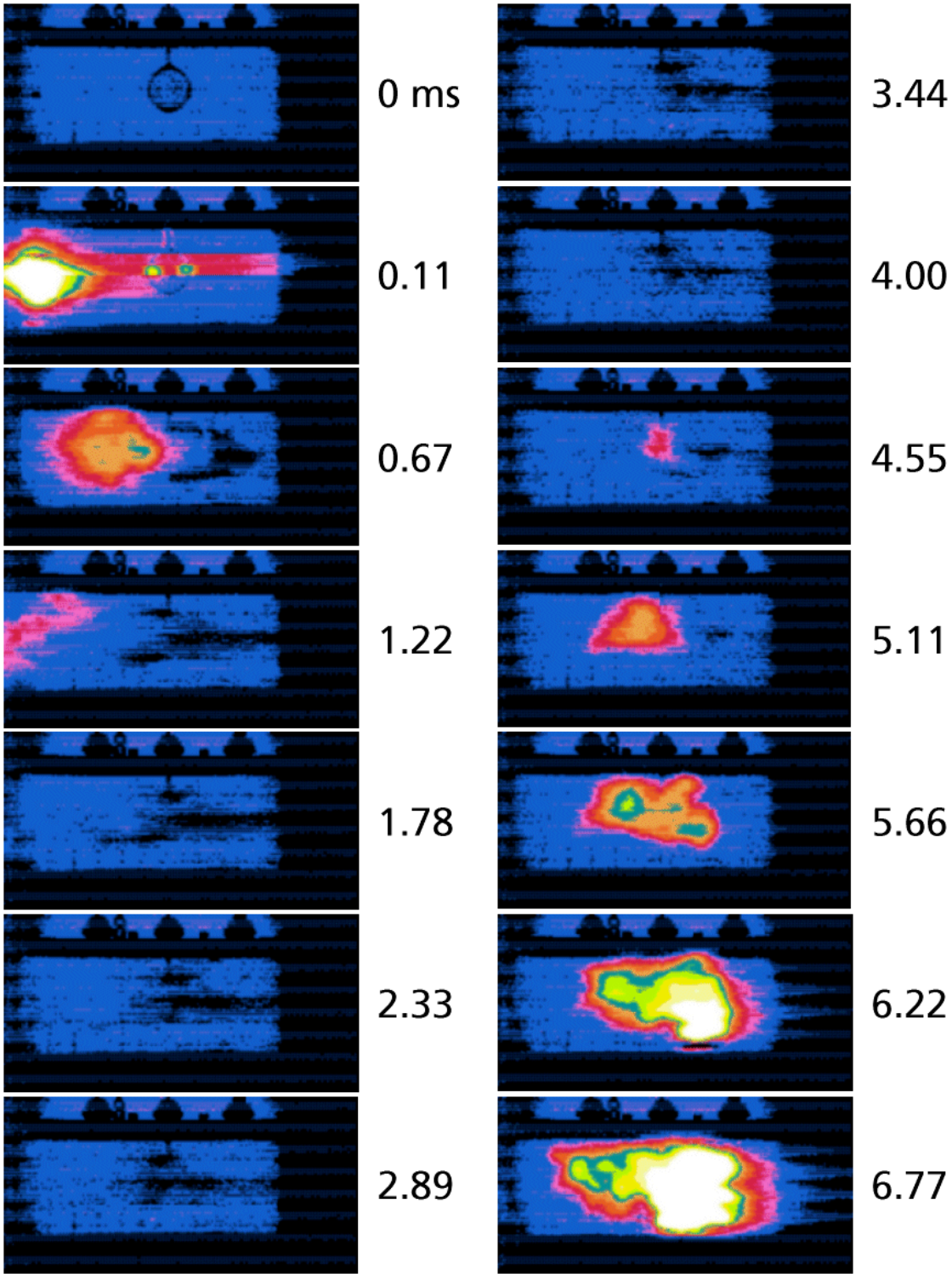

Figure 5. Sequence of pseudo-color high-speed photographs depicting the hot detonation and combustion products in the chamber.

3. Model

3.1 Conservation Laws

The Model is based on the Eulerian multi-phase conservation laws for a dilute heterogeneous continuum [6]. We model the evolution of the gas phase combustion fields in the limit of large Reynolds and Peclet numbers, where effects of molecular diffusion and heat conduction are negligible. The flow field is governed by the gas-dynamic conservation laws:

Mass: $$\partial_t \rho + \nabla \cdot (\rho \mathbf{u}) = \dot{\sigma}_s \tag{1}$$

Momentum: $$\partial_t \rho \mathbf{u} + \nabla \cdot (\rho \mathbf{u}\mathbf{u} + p) = \dot{\sigma}_s \mathbf{v} - \dot{f}_s \tag{2}$$

Energy: $$\partial_t \rho E + \nabla \cdot (\rho \mathbf{u} E + p\mathbf{u}) = -\dot{q}_s + \dot{\sigma}_s E_s - \dot{f}_s \cdot \mathbf{v} \tag{3}$$

where ρ, p, u represent the gas density, pressure and specific internal energy, $\mathbf{u}$ is the gas velocity vector, and $E \equiv u + \mathbf{u} \cdot \mathbf{u}/2$ denotes the total energy of the gas phase. Source terms on the right hand side take into account: mass addition to gas phase due to particle burning ($\dot{\sigma}_s$), particle drag ($\dot{f}_s$), and heat losses ($\dot{q}_s$).

We treat the particle phase as a Eulerian continuum field [6,7]. We consider the dilute limit, devoid of particle-particle interactions, so that the pressure and sound speed of the particle phase are zero. We model the evolution of particle phase mass, momentum and energy fields by the conservation laws of continuum mechanics for heterogeneous media:

Mass: $$\partial_t \sigma + \nabla \cdot \sigma \mathbf{v} = -\dot{\sigma}_s \tag{4}$$

Momentum: $$\partial_t \sigma \mathbf{v} + \nabla \cdot \sigma \mathbf{v}\mathbf{v} = -\dot{\sigma}_s \mathbf{v} + \dot{f}_s \tag{5}$$

Energy: $$\partial_t \sigma E_s + \nabla \cdot \sigma E_s \mathbf{v} = \dot{q}_s - \dot{\sigma}_s E_s + \dot{f}_s \cdot \mathbf{v} \tag{6}$$

where σ and $\mathbf{v}$ represent the particle-phase density and velocity and $E_s \equiv C_s T_s$ denotes the energy of the particle phase.

3.2 Interactions

The inter-phase interaction terms for mass, momentum, and heat take the form as described by Khasainov [8]:

Mass Exchange: $$\dot{\sigma}_s = \begin{cases} 0 & T_s < T_{melt} \\ -3\sigma(1 + 0.276\sqrt{\mathrm{Re}_s})/t_s & T_s \geq T_{melt} \end{cases} : \tag{7}$$

Momentum Exchange: $$\dot{f}_s = (3\rho\sigma/4\rho_s d_s) C_D (\mathbf{u} - \mathbf{v})|\mathbf{u} - \mathbf{v}| \tag{8}$$

Heat Exchange: $$\dot{q}_s = (6\sigma/\rho_s d_s)\left[Nu\lambda(T - T_s)/d_s + \varepsilon\sigma_{Boltz}(T^4 - T_s^4) \right] \tag{9}$$

Burning Law: $$t_s = K d_{s0}^2 \tag{10}$$

where $C_D = 24/\mathrm{Re}_s + 4.4/\sqrt{\mathrm{Re}_s} + 0.42$, $\mathrm{Re}_s = \rho d_s |\mathbf{u} - \mathbf{v}|/\mu$ and $Nu = 2 + 0.6\,\mathrm{Pr}\sqrt{\mathrm{Re}_s}$. Here, we assume the mass transfer from particles to continuum occurs a the melting point of Al and we view the Al in the continuum phase as a micro-mist of Al droplets in velocity and thermal equilibrium wit the gas but does not contribute to pressure. An additional phase change is included at the vaporization temperature of Al, at which point it becomes a gas and contributes to the gas pressure.

3.3 Combustion

We consider three fuels: *C4* detonation products (F_1), Aluminum (F_2), and gaseous hydrocarbon (F_3), along with their corresponding combustion products: *C4*-air (P_1) and Al-air (P_2) and C_2H_2 – air (P_3). (Al is assumed to only burn in the continuum phase). We consider global combustion of fuel F_k with air (A) producing equilibrium combustion products P_k:

$$F_k + A \Rightarrow P_k \qquad (k = 1,\ 2 \text{ or } 3) \tag{11}$$

The mass fractions Y_k of the components are governed by the following conservation laws:

Fuel-k: $$\partial_t \rho Y_{Fk} + \nabla \cdot \rho Y_{Fk}\mathbf{u} = -\dot{s}_k + \delta_{k2}\dot{\sigma}_k \tag{12}$$

Air: $$\partial_t \rho Y_A + \nabla \cdot \rho Y_A \mathbf{u} = -\sum_k \alpha_k \dot{s}_k \tag{13}$$

Products-k: $$\partial_t \rho Y_{Pk} + \nabla \cdot \rho Y_{Pk}\mathbf{u} = \sum_k (1+\alpha_k)\dot{s}_k \tag{14}$$

Fuel and air are consumed in stoichiometric proportions: $\alpha_k = A/F_k$. In the above, $\dot{s}_k$ represents the global kinetics sink term. In this work we use the fast-chemistry limit that is consistent with the inviscid gas-dynamic model (1)-(3), so whenever fuel and air enter a computational cell, they are consumed in one time step. Here δ_{k2} represents the Kronecker delta ($\delta_{k2} = 0$ if $k \neq 2$ and $\delta_{k2} = 1$ if $k = 2$) and takes into account the mass transfer of Al from the particle phase EQ. (4) to the gas phase.

3.4 Equations of State

The thermodynamic states encountered during SDF explosions have been analyzed in by Kuhl and Khasainov [9]. The loci of states of component c in the specific internal energy-temperature ($u-T$) plane (Fig. 6) are fit with quadratic functions of temperature:

$$u_c(T) = a_c T^2 + b_c T + c_c \tag{15}$$

For cells containing a mixture of components, the mixture energy also satisfies a quadratic form:

$$u_m(T) = \sum_c Y_c u_c = a_m T_m^2 + b_m T_m + c_m \tag{16}$$

Given the mixture specific internal energy u_m, the mixture temperature can be evaluated by:

$$T_m = [-b_m + \sqrt{b_m^2 - 4a_m(c_m - u_m)}\,]/2a_m \tag{17}$$

using mixture coefficients as defined by:

$$a_m = \sum_c Y_c a_c\,,\; b_m = \sum_c Y_c b_c\,,\; c_m = \sum_c Y_c c_c\,,\; R_m = \sum_c Y_c R_c \tag{18}$$

For pure cells, the pressure of a component is calculated from the perfect gas relation $p_c = \rho_c R_c T_c$, or from the JWL function in the detonation products gases [4]. In mixed cells, the pressure is calculated from the mixture temperature by the "law of additive pressures":

$$p_m = \sum_c p_c(V_m, T_m) \tag{19}$$

where $p_c(V_m, T_m)$ denotes the pressure of component c if it existed alone at V_m and T_m.

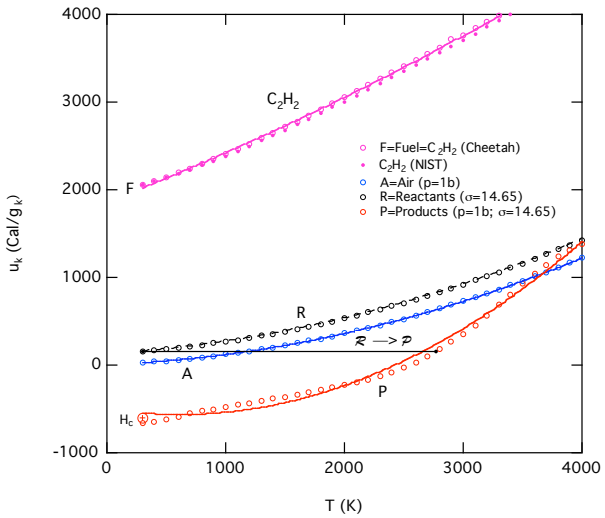

Figure 6. Le Chatelier diagram of internal energy, u_k, versus temperature, T, for combustion of acetylene (C_2H_2) in air based on thermodynamic calculations using the Cheetah code. Points *A* denotes air, while *F* represents fuel of fixed composition. These combine in stoichiometric proportions (air-fuel ratio: $\sigma = 14.65$) to form reactants *R* (of fixed composition) and equilibrium products *P*.

3.5 Numerical Methods

The governing equations (1)-(6) and (12)-(14) are integrated with high-resolution upwind methods that represent high-order generalizations of Godunov's method. The algorithm for gas phase conservation laws is based on an efficient Riemann solver for gas-dynamics first developed by Colella and Glaz [10]. The algorithm for the particle phase conservation laws is based on a Riemann solver for two-phase flows developed by Collins et al. [11]. Source terms are treated with operator splitting methods. Being based on Riemann solvers, information propagates along characteristics at the correct wave speeds, and they incorporate nonlinear wave interactions within the cell during the time step.

These Godunov schemes have been incorporated into the embedded boundary adaptive mesh refinement (AMR) algorithm of Pember et al. [12] that allows us to focus computational effort in complex regions of the flow such as mixing layers and reaction zones. In this AMR approach, regions to be refined are organized into rectangular patches, with 100's to 1,000's of grid-points per patch. AMR is also used to refine turbulent mixing regions; by successive refinements we are able to capture the energy-bearing scales of the turbulence on the computational grid. In this way we are able to compute the effects of turbulent mixing without resorting to turbulence modeling (which is not applicable to this problem). This is consistent with the "MILES" approach of Boris et al. [13].

4. Results

The two-phase AMR code was used to simulate the combustion of the acetylene cloud of the experiment shown in Fig. 5. Computed pressure histories (Fig. 7) are in excellent agreement with the data—thereby proving the validity of our modeling hydrocarbon-air combustion in explosions.

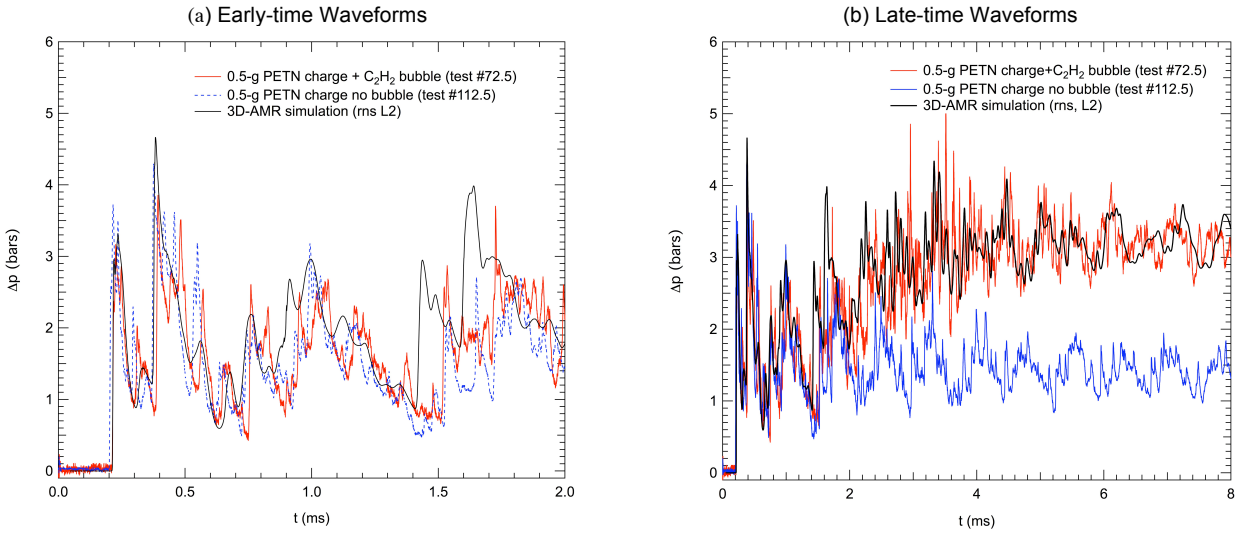

Figure 7. Pressure histories at gauge 5 for a 0.5-g spherical PETN charge detonated in the tunnel filled with air. Case 1: with an acetylene bubble (d = 50 mm), Case 2: no bubble; Case 3: 3D-AMR code simulation.

Next the two-phase AMR code was used to simulate the combustion of an acetylene cloud in an SDF explosion. The problem configuration was similar to that shown in Fig. 3: a 1.5-g SDF charge (consisting of 0.5-g spherical PETN booster surrounded by 1 g of flake Aluminum powder) located at x = 9.65 cm and a spherical acetylene cloud (d = 5 cm) located at x = 26.8 cm in the rectangular tunnel. The evolution of the reactive blast wave from the SDF charge is shown in Fig. 8. The explosion products cloud temperature ranges from 3,000 K to 4,000 K[1] as a consequence of combustion with air. The blast wave reaches the cloud at 120 μs. The ignition, mixing and combustion of the acetylene cloud with air are shown Fig. 9. The cloud products can reach temperatures of 2,775 K (the adiabatic flame temperature of C_2H_2-air) and even as high as 4,000 K (red zones) due to turbulent mixing with the hot Al-air combustion products gases.

[1] see Appendix for temperature color bar.

(a) t = 0 μs

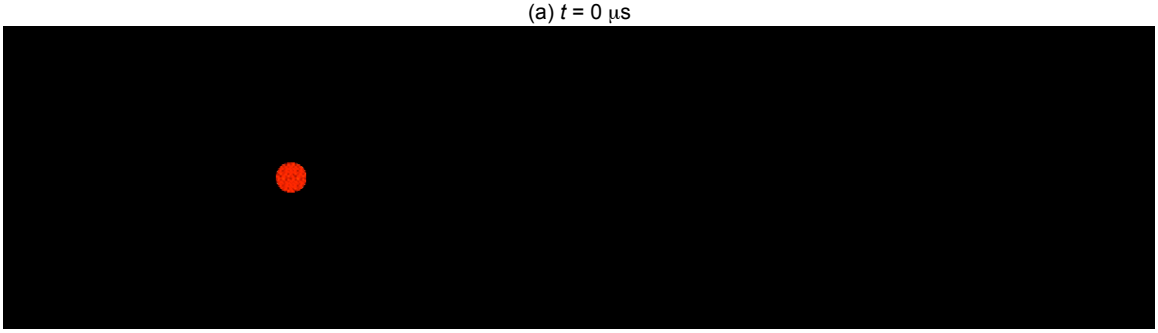

(b) t = 31 μs

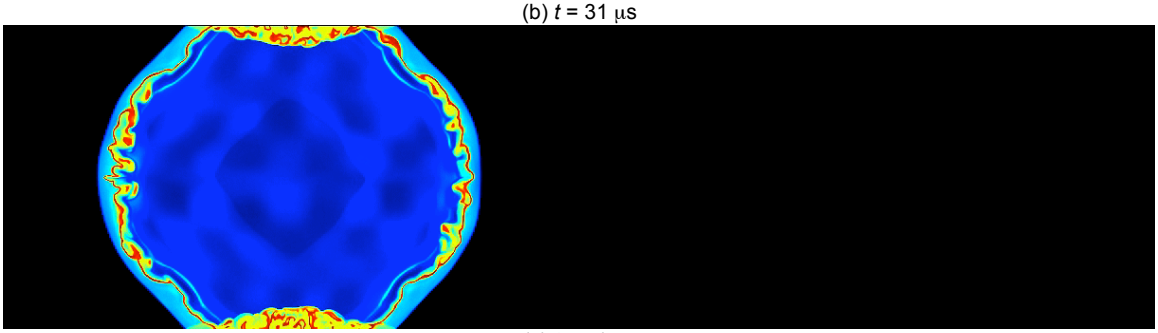

(c) t = 51 μs

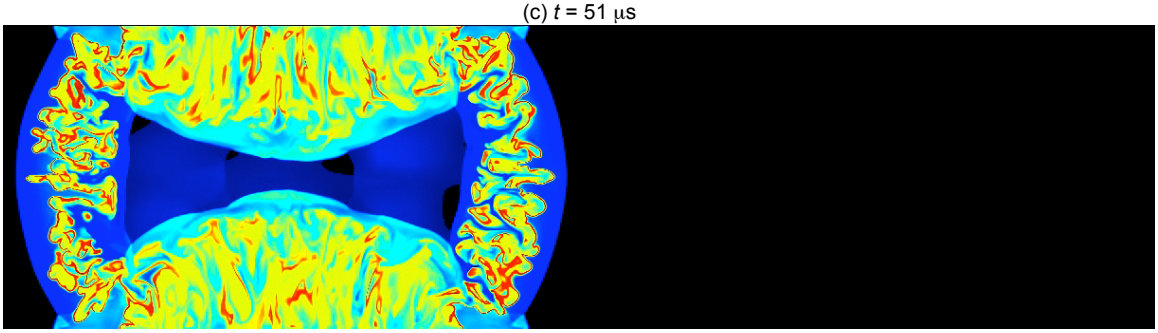

(d) t = 118 μs

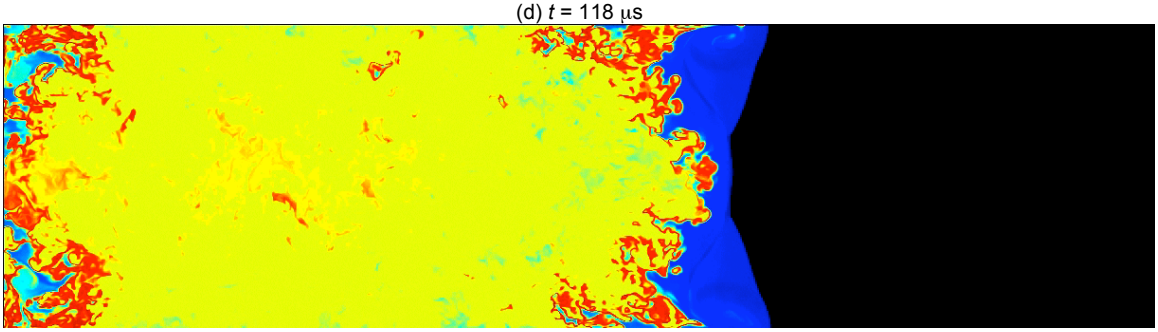

(e) t = 203 μs

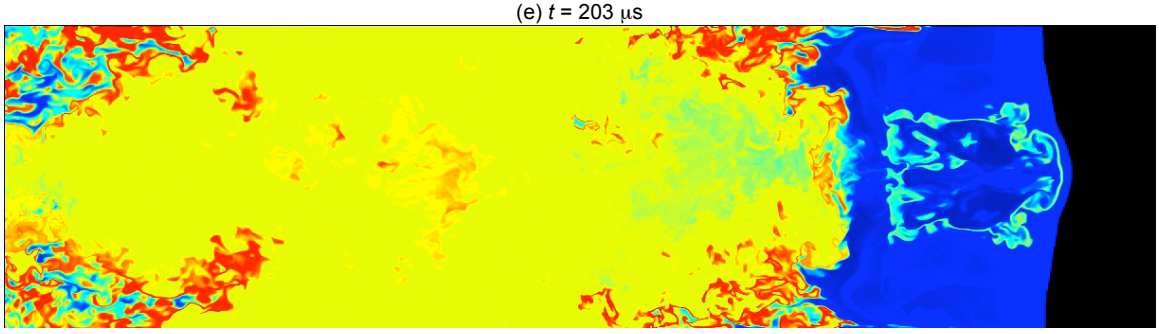

Figure 8. Cross-section of the temperature field from 1.5-g Al-SDF charge explosion in a tunnel.
(red = 4,500K, yellow = 3,000K, turquois = 2,000K and blue = 300K; see color bar in Appendix)

(f) t = 360 μs

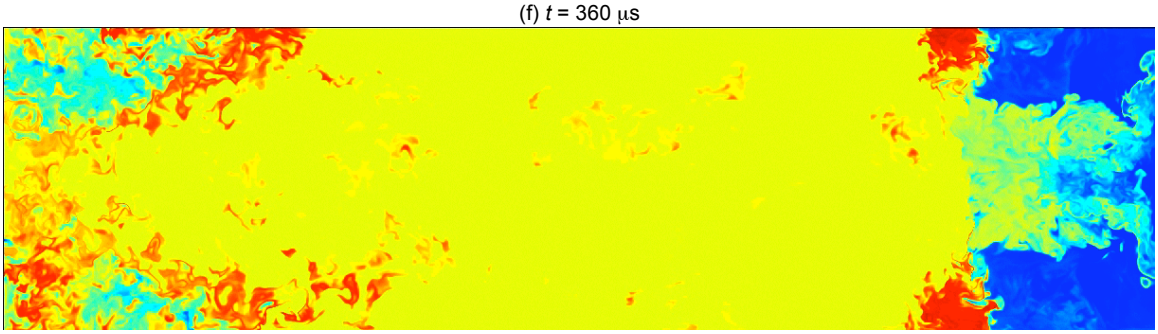

(g) t = 551 μs

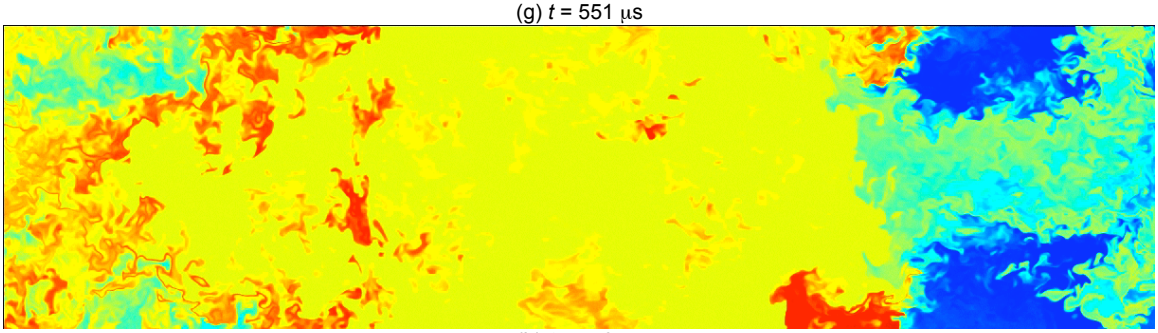

(h) t = 756 μs

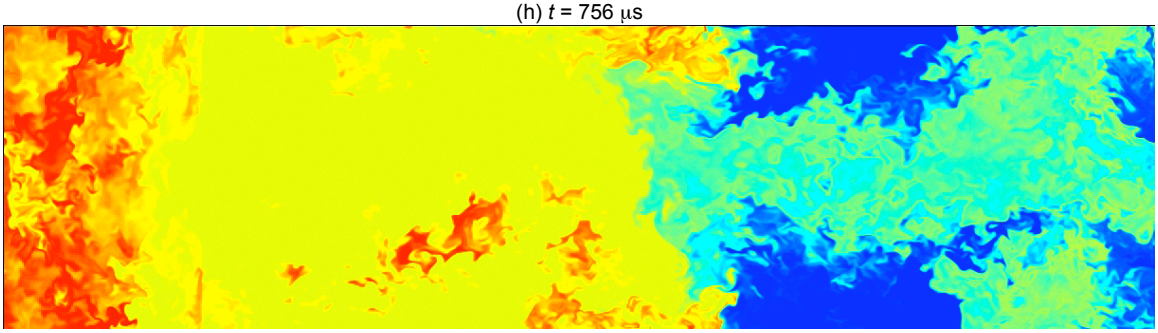

(i) t = 1,000 μs

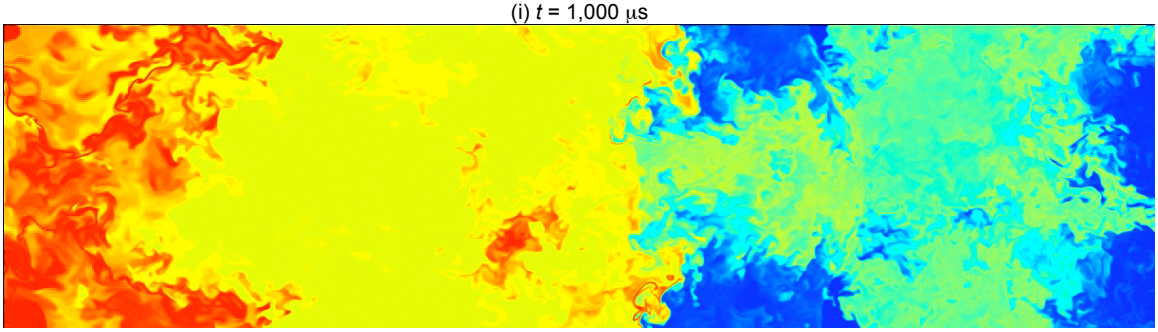

(j) t = 1,273 μs

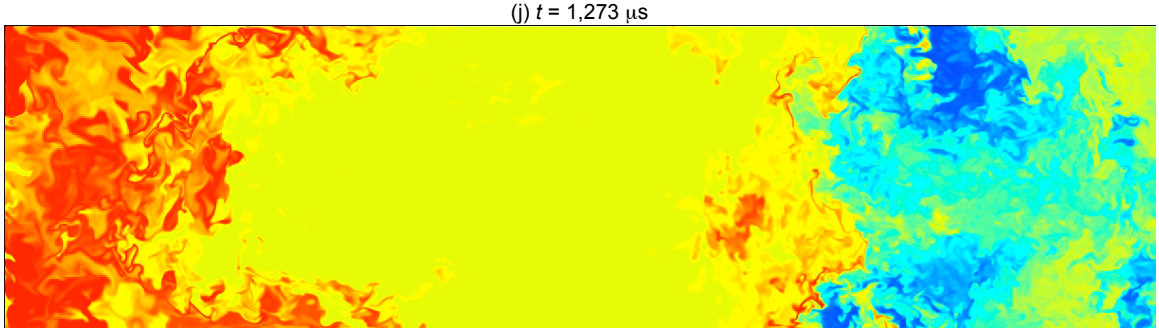

Figure 8. Concluded (see color bar in Appendix).

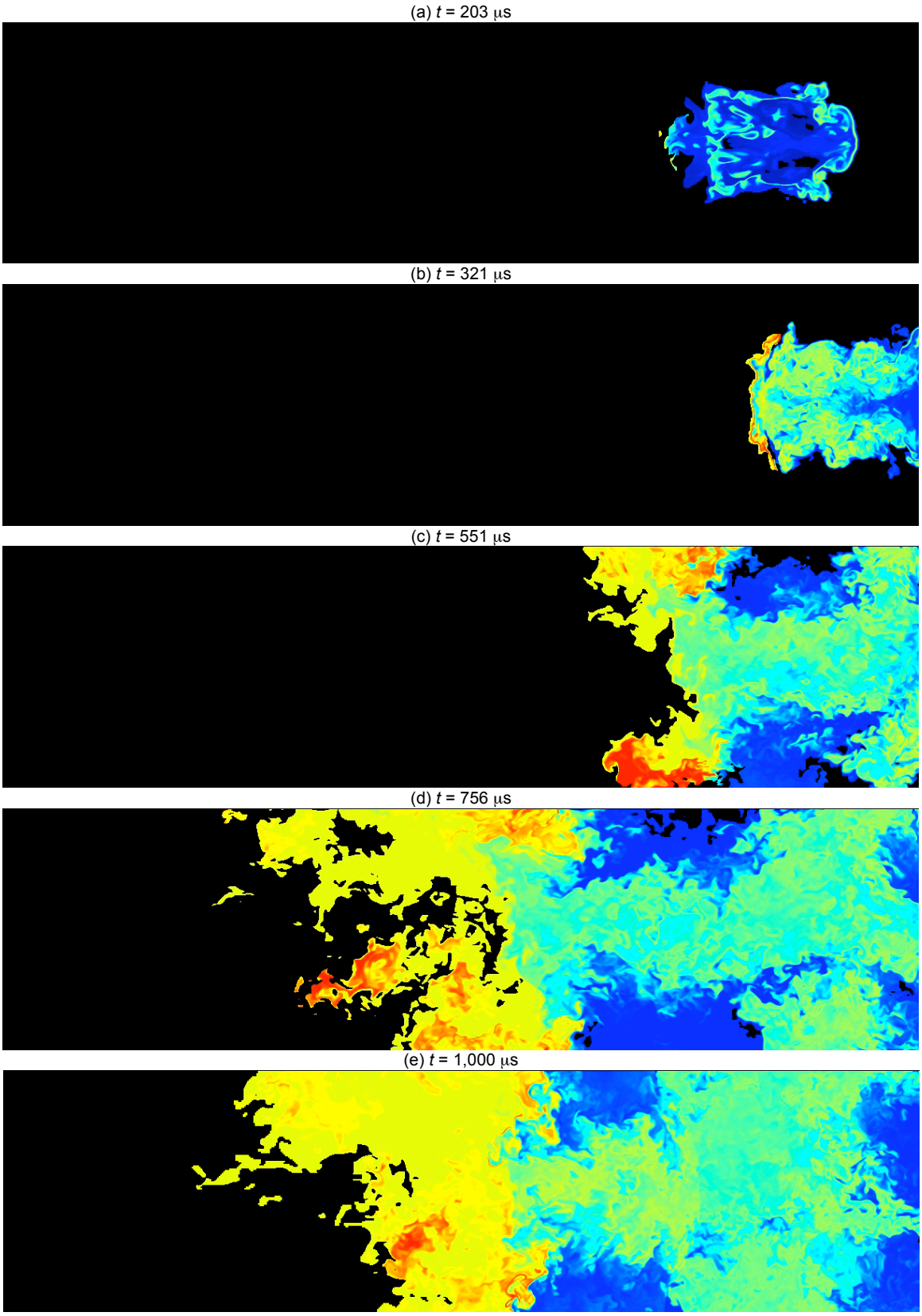

Figure 9. Cross-section of the temperature field of the acetylene cloud combustion in a tunnel (acetylene cloud mass is visualized: red = 4,500K, yellow = 3,000K, turquois = 2,000K and blue = 300K; see color bar in Appendix).

Evolution of the global mass histories are presented in Fig. 10. There one can see the formation of the Al fuel (due to melting of Al powder) and the consumption of the fuels in Fig. 10(a). And one can observe the formation of products masses due to combustion with air in Fig. 10(b). Consumption of the acetylene cloud mass fraction, $\mu_c(t) \equiv m_c(t)/m_c(0)$, is depicted in Fig. 11; by a time of 1.3 ms, only 15% of the acetylene mass remains.

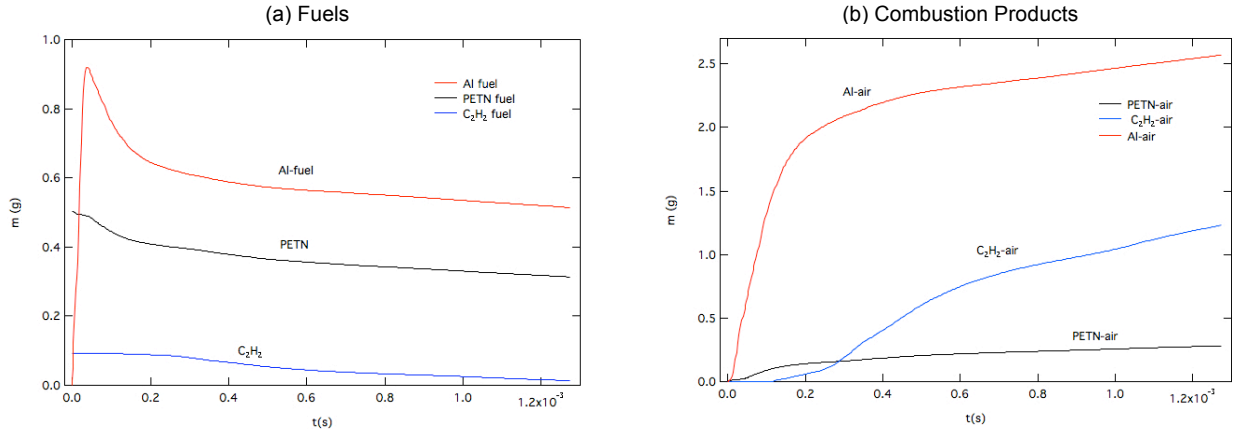

Figure 10. Evolution of the global mass histories

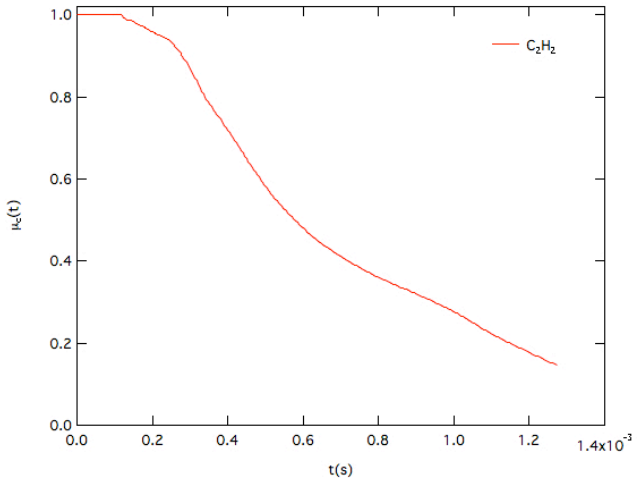

Fig. 11. Acetylene cloud mass fraction versus time.

5. Conclusions

A heterogeneous continuum model of Al particle combustion in explosions has been developed. It has been extended to model hydrocarbon cloud combustion in such explosion fields. The model has been validated by comparison with experiments of acetylene cloud combustion in a 4-liter tunnel. Next it was used to simulate acetylene cloud combustion induced by a 1.5-g Al-SDF explosion in the same tunnel. The SDF products cloud temperature ranged from 3,000 K to 4,000 K. The acetylene products temperature ranged from 2,775 K (adiabatic flame temperature) to 3,000 K (due to mixing with the hot SDF products gases). By 1.3 ms, more than 85 % of the acetylene cloud mass had been consumed by combustion. Future work will explore the effects of detailed kinetics on the combustion process.

References

[1] Kuhl, A. L, Reichenbach, H. (2008) Combustion effects in confined explosions, *Proc. Combustion Inst.* **32** (2009) pp 2291-2298.

[2] Bell, J. B., Beckner, V. E. & Kuhl, A. L. (2007) Simulation of enhanced explosive devices in chambers and tunnels (plenary lecture), *DOD High Performance Computing Users Group Conf. 2007 (HPCMP-UGC 2007) 0-7695-3088-5/07 IEEE*, 5 pp.

[3] Kuhl, A. L., Bell and J. B, Beckner, V. E. (2009) AMR Code Simulations of Turbulent Combustion in Confined and Unconfined Explosions, *HPCMP-UGC 2009, IEEE*, 6 pp.

[4] Glaude, P. A., Melius, C., Pitz, W. J., and Westbrook, C. K. (2002) Detailed Chemical Kinetic Reaction Mechanisms of Incineration of Organophosphorus & Flurorganophosphorus Compounds, *Proc. Comb. Inst.*, **29**, 2469-2476, 2002.

[5] Neuwald, P., Reichenbach, H. and Kuhl, A.L. (2001) Explosion induced combustion of hydrocarbon clouds in a chamber, *18th Int. Colloquium on Dynamics of Explosions and Reactive Systems*, Seattle, WA, 6 pp.

[6] Kuhl, A.L., Bell, J. B. and Beckner, V.E. (2009) Heterogeneous continuum model of Aluminum particle combustion in explosions, *Fizika Goreniya i Vzryva* (in press).

[7] Nigmatulin, R. I. (1987) *Dynamics of Multi-Phase Flows.* Vol. 1. Moscow, Nauka, 464 pp.

[8] Veyssiere, B., and Khasainov, B. (1991) A Model for steady, Plane, double-front detonations (DFD) in gaseous explosive mixtures with aluminum particles in suspension, *Combustion and Flame* Vol. 85 (1, 2), 1991, pp. 241-253.

[9] Kuhl, A. L. and Khasainov, B. (2007) Quadratic model of thermodynamic states in SDF explosions, *Energetic Materials: 38th Int. Conf. ICT*, pp. 143.1-143.11.

[10] Colella, P. and Glaz, H. M. (1985) Efficient solution algorithms for the Riemann problem for real gases", *J Comp. Phys.,* 59, pp. 264-289.

[11] Collins, P., Ferguson, R. E., Chien, K. Kuhl, A.L., Krispin, J. and Glaz, H. M. (1994) Simulation of shock-induced dusty gas flows using various models, AIAA 94-2309.

[12] Pember, R. B., Bell, J. B., Colella, P., Crutchfield, W. Y. and Welcome, M. L. (1995) An Adaptive cartesian grid method for unsteady compressible flow in irregular regions, *J. Comp. Phys.*, 120:2, pp. 278-304, 1995.

[13] Boris, J. P., Grinstein, F. F., Oran, E. S., & Kolbe, R. L. (1992) New insights into large eddy simulation, *Fluid Dynamics Research*, 10.

ACKNOWLEDGEMENTS

This work performed under the auspices of the U.S. Department of Energy by Lawrence Livermore National Laboratory under Contract DE-AC52-07NA27344. The work at LBNL was performed under U.S. Department of Energy under Contract No. DE-AC02-05CH11231. This work was sponsored by the Defense Threat Reduction Agency under IACRO's 08-4399l, 09-45091 and 10-4966I; Dr. William Wilson, DTRA/CXWJ, is the contract monitor; his support is greatly appreciated.

Appendix

Quadratic model for acetylene-air combustion

$$u_A(T) = 7.358 + 0.049652*T + 6.3348*10^{-5}*T^2 \quad u_F(T) = 1858.8 + 0.52781*T + 3.478*10^{-5}*T^2$$

$$u_R(T) = 125.66 + 0.080205*T + 6.1523*10^{-5}*T^2 \quad u_P(T) = -499.54 - 0.21052*T + 17.185*10^{-5}*T^2$$

The calculated heat of combustion $\Delta u = -773.97\ Cal/g_P$ is in good agreement with the value ΔH_c^0 = -722.6 Cal/g_p = (-11,308 Cal/g_{C2H2})/(1 + σ) published for acetylene (NBS, 1952). The standard energies are: E_{0,C_2H_2} = 2,2059.97 $Cal/g_{C_2H_2}$, $E_{0,Air} = -20.54\ Cal/g_{Air}$, $E_{0,P} = 112.42\ Cal/g_P$.

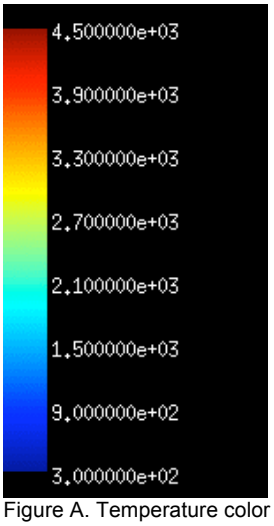

Figure A. Temperature color palette.